The volitional control of individual motor units is constrained within low-dimensional manifolds by common inputs

Julien ROSSATO[1,2], Simon AVRILLON[3], Kylie TUCKER[4],
Dario FARINA[3] and François HUG[4,5]*

[1] Nantes Université, Laboratory "Movement, Interactions, Performance" (UR 4334), Nantes, France
[2] IRCCS Fondazione Santa Lucia, Laboratory of Neuromotor Physiology, Rome, Italy.
[3] Department of Bioengineering, Faculty of Engineering, Imperial College London, London, United Kingdom.
[4] The University of Queensland, School of Biomedical Sciences, Brisbane, QLD, Australia
[5] Université Côte d'Azur, LAMHESS, Nice, France

* Corresponding author
Prof. François Hug
Université Côte d'Azur, LAMHESS, Nice, France
Francois.hug@univ-cotedazur.fr

Running title: Low-dimensional control of motor units

Supplemental data availability: The entire dataset (raw and processed data) and codes will be made available upon publication.

Conflict of interests: The authors declare no competing financial interests.

Funding resources: François Hug is supported by the French government, through the UCAJEDI Investments in the Future project managed by the National Research Agency (ANR) with the reference number ANR-15-IDEX-01 and by an ANR grant (ANR-19-CE17-002-01, COMMODE project). Dario Farina is supported by the European Research Council Synergy Grant NaturalBionicS (contract #810346), the EPSRC Transformative Healthcare, NISNEM Technology (EP/T020970), and the BBSRC, "Neural Commands for Fast Movements in the Primate Motor System" (NU-003743).

Author Contributions:
Contribution and design of the experiment: JR, SA, DF, FH; Collection of data: JR; Analysis and interpretation: JR, SA, KT, DF, FH; Drafting the article or revising it for important intellectual content: JR, SA, KT, DF, FH; All authors approved the final version of the manuscript.

Abstract.

The implementation of low-dimensional movement control by the central nervous system has been debated for decades. In this study, we investigated the dimensionality of control signals received by spinal motor neurons in controlling one degree of freedom of either the ankle or knee joint. We hypothesized that the central nervous system would mainly adopt a rigid control of motor units; specifically, that the motor units active during these tasks would belong to a small number of synergies, each receiving common descending inputs. This hypothesis was tested using torque-matched isometric contractions, as well as with an operant-conditioning paradigm, where the firing activities of pairs of motor units were provided as visual feedback to the participants. The motor units of the gastrocnemius lateralis could be controlled largely independently from those of the gastrocnemius medialis during ankle plantarflexion. This dissociation of motor unit activity imposed similar behavior to the motor units that were not displayed in the feedback, leading to a two-dimensional control manifold, where each dimension represented a "synergistic" muscle. It was not possible to independently control the motor units within the gastrocnemius medialis muscle. During knee extension tasks, it was not possible to dissociate the activity of the motor units between the vastus lateralis and medialis muscles, which thus belonged to a one-dimensional manifold. Overall, individual motor units were never controlled independently of all others but rather belonged to synergistic groups. These results provide evidence for a synergistic low-dimensional control of motor units constrained by common inputs spanning one or more muscles.

Keywords: electromyography; synergies; modules; motor neurons; real-time feedback.

Introduction.

To generate movement, the central nervous system must provide appropriate inputs to the spinal motor neurons, which are the final common pathway of the neuromuscular system [1]. The relatively large number of spinal motor neurons (e.g., >20,000 to control the upper limbs [2]) implies a control space of high dimensionality. How the central nervous system navigates through this high-dimensional space to generate neural commands for the muscular system remains an open question [3,4].

Observations from the motor areas of the cortex [5] and the spinal cord [6,7] have led to the view that the central nervous system relies on neuronal population coding rather than single neuron coding to control movements. This is supported by studies reporting correlations between the firing activity of spinal motor neurons that innervate the same or different muscles [8-12]. As the outputs of two motor neurons cannot be correlated without a certain degree of correlation in their inputs [13], this correlated activity underlies the common inputs received by the motor neurons. However, a precise quantification of this common input is not possible because of the nonlinear input-output function of motor neurons [14].

The control of motor neurons by common inputs aligns with the synergy hypothesis [3], which proposes that a small number of inputs project to a greater number of controlled structures through specific neural circuits [15-17]. In this view, large groups (synergies) of motor neurons would share common inputs that constrain their firing behavior within a low-dimensional manifold, which is mainly invariant across motor tasks. This suggests that the central nervous system operates in a control space that is much smaller than the number of motor neurons. This control strategy can also leverage automatic low-level control mechanisms that emerge from the combination of common inputs and intrinsic motor neuron properties. An example is the orderly recruitment following the size principle [18], observed in motor neurons receiving the same inputs. Finally, while computationally efficient, this strategy would impose some "rigidity" in the control of motor neurons as motor neurons within the same synergy would always receive the same inputs and therefore would always be activated in the same order.

An alternative hypothesis to hardwired neural synergies suggests that common inputs to motor neurons are the result of the optimization of high-level policies to complete a specific task while minimizing, for example, the effect of synaptic noise on motor output [19,20]. From this

perspective, the central nervous system can flexibly modify the distribution of common inputs to motor neurons across motor tasks. This implies that motor neurons may belong to different synergies during different tasks.

In this study, we hypothesized that the central nervous system mainly adopts a rigid control of the motor units, at least during a motor task with a single mechanical degree of freedom, and without extensive learning. We tested this hypothesis by selecting pairs of motor units based on their anticipated level of common inputs in reference conditions, considering i) motor units from the same muscle (gastrocnemius medialis; GM-GM) and the same motor neuron synergy [21], ii) motor units from different muscles (vastus lateralis and medialis; VL-VM) but from the same synergy [10], and ii) motor units from different muscles (gastrocnemius lateralis and medialis; GL-GM) and different synergies [21]. We first assessed the association between the firing of target motor units during torque-matched isometric contractions. Subsequently, we evaluated the extent to which the same motor units could be independently controlled using an operant-conditioning paradigm in which participants received the corresponding motor unit firing rates as real-time feedback. This biofeedback paradigm, pioneered by Basmajian [22], was previously used to study flexible/rigid control by Formento et al. [23] and Bracklein et al. [24], with conflicting results. These conflicting observations may reflect different baseline mappings of common inputs to motor units, which have not been systematically assessed in these previous studies. We assumed that the activity trajectory of two motor units receiving a common input would be constrained to a monotonic one-dimensional manifold [25]. Therefore, the rigid control that we hypothesized implies that the activity of two motor units receiving common descending inputs cannot be dissociated with operant conditioning. By extension, the activities of two motor units receiving different descending inputs can be volitionally dissociated with no effort. This approach provides evidence of the flexibility or rigidity of the volitional control of motor units, because of the freedom to explore different inputs to motor neurons using the operant-conditioning paradigm.

We found that the activity of most motor unit pairs from the GL and GM could be volitionally controlled and dissociated, imposing a similar behavior to that of the non-displayed units, i.e. at the population level. However, such a dissociation was not systematically observed for the other pairs of motor units from the same (GM-GM) or different muscles (VL-VM). Moreover, the flexible volitional control of individual motor units with respect to all others has never been observed. Together, our results provide evidence of a low-dimensional control of motor units

constrained by common inputs spanning one or several muscles, which drastically limits the level of flexibility in motor unit recruitment.

Results.

Fifteen participants performed either isometric plantarflexion (n = 10) or knee extension tasks (n = 5) with visual feedback of either the generated effective torque (first part) or the firing rate of two motor units (second part). Electromyographic (EMG) signals were recorded using surface grids of 64 electrodes from the GL and GM muscles during plantarflexion tasks and from the VL and VM muscles during knee extension tasks. We used a source-separation algorithm to decompose the EMG signals into motor unit discharge times either offline or in real-time using an open-source software developed and validated by our team[26].

Behavior of motor units during contractions with torque feedback

In the first part of the experiment, participants were instructed to perform ten 15 s isometric contractions at a submaximal level of torque (10-25% of the maximal voluntary contraction [MVC] torque, depending on the participant, see *Methods*), referred to as "reference" contractions (Figure 1A). This experimental part aimed to describe the synergistic behavior of motor units at the population level during single-joint isometric contractions, in which the participants only received *torque* feedback.

Participants accurately tracked the target torque with a root mean square error of 0.4 ± 0.1% (plantarflexion) and 0.3 ± 0.1% (knee extension). We identified a total number of 40 (GL), 110 (GM), 34 (VL), and 15 (VM) motor units. The smoothed firing rate of the identified motor units was estimated during the plateaus of force of the 10 contractions, and the cross-correlation between these smoothed firing rates was assessed for all pairs of motor units (Figure 1B). The correlation coefficients were compared using a linear mixed effect-models with Muscle (GL-GM, GM-GM, and VL-VM) as a fixed factor and Participants as a random factor. A muscle effect ($F = 24.1$; $p < 0.001$) was observed, with lower correlation coefficients for pairs of motor units from GL and GM (0.80 ± 0.20) than for pairs from GM (0.90 ± 0.20; $p < 0.001$) and from VL and VM (0.96 ± 0.009; $p = 0.032$). No significant differences were observed between the GM-GM pairs and VL-VM pairs ($p = 0.66$). We then identified the percentage of pairs of motor units with significant correlations. The significance threshold was considered as the 95th percentile of the distribution of correlation coefficients computed for 100 pairs of synthetic motor units with a random series of firings generated by bootstrapping the inter-spike intervals of the original motor units. When considering pairs of motor units from the GM muscle, the percentage of pairs exhibiting significant correlations reached 98.3 ± 5.3% (GM-GM) (Figure

1B). The percentage was lower when considering pairs of motor units from different muscles: 85.6 ± 13.4% (GL-GM) and 84.2 ± 18.3% (VL-VM; Figure 1B).

We further investigated whether the behavior of the motor unit pairs was compatible with the existence of a 1-D common input using two metrics proposed by Marshall et al. [25]: *motor unit displacement* and *dispersion* (Figure 1C). These metrics consider that the firing rate of two motor units receiving a 1-D common input should vary along a 1-D monotonic manifold, with the firing rate of both units increasing or decreasing when the synaptic input increases or decreases, respectively (e1 in Figure 1C). In some cases, the firing rate of one unit can increase while the other one stays at 0 because of a higher recruitment threshold (e2 in Figure 1C), or remains at the same value due to rate saturation (e3 in Figure 1C). Any deviation from these cases would oppose the hypothesis of a 1-D common input. The *motor unit displacement* quantifies the difference in firing rates between two motor units when the firing rates of the two units vary in opposite directions (one increases, and one decreases; e4 in Figure 1C). Following the same rationale as that described above, the firing rates of a population of motor units should also vary along a 1-D monotonic manifold. Therefore, the summed firing rates of this population of motor units, equivalent to its L1-norm, should always be associated with the same population state: that is, the distribution of firing rates within the population, across contractions. Any change in the distribution of firing rates within a population of motor units for a given norm value λ would also contradict the hypothesis of a 1-D common input. The *dispersion* quantifies the maximal difference between the L1-norms for a given norm value λ (λ = 14 in Figure 1C). The higher the *displacement* and *dispersion*, the higher the deviation from the 1-D monotonic manifold, as depicted in typical examples of state spaces for two pairs of motor units from the GL-GM and VL-VM in Figure 1C.

Motor unit displacement and dispersion were computed over the 10 reference contractions for the populations of identified motor units, i.e. for motor units from the GL and GM, from GM only, and from VL and VM. These metrics were compared using a linear mixed-effects model with Muscle (GL-GM, GM-GM, and VL-VM) as a fixed factor and Participants as a random factor. There was a main effect of Muscle ($F = 10.9$; $p = 0.001$) on motor unit displacement, which was higher for motor units from GL-GM (10.4 ± 2.7 pps) than for those from GM (7.6 ± 2.4 pps; $p = 0.003$); with no other differences (all p values > 0.19; Figure 1D). A main effect of Muscle ($F = 10.9$; $p = 0.001$) was also found for the dispersion, which was significantly

higher for the populations of motor units from GL-GM (60.1 ± 26.7 pps) than for those from GM (32.7 ± 19.3 pps; $p = 0.004$) and VL-VM (17.2 ± 6.9 pps; $p = 0.048$; Figure 1D). No significant differences were identified between GM-GM and VL-VM ($p = 0.98$).

Overall, these results indicate that during a mechanically constrained task, in which the participants match an effective torque, most of the pairs of motor units exhibit a high level of correlation between their smoothed firing rates, with higher flexibility between motor units from the GL-GM than from the VL-VM and GM-GM. To determine whether these results reflect neural constraints on motor unit firing activity, participants were asked to volitionally dissociate the firing rates of motor units in the second part of the experiment.

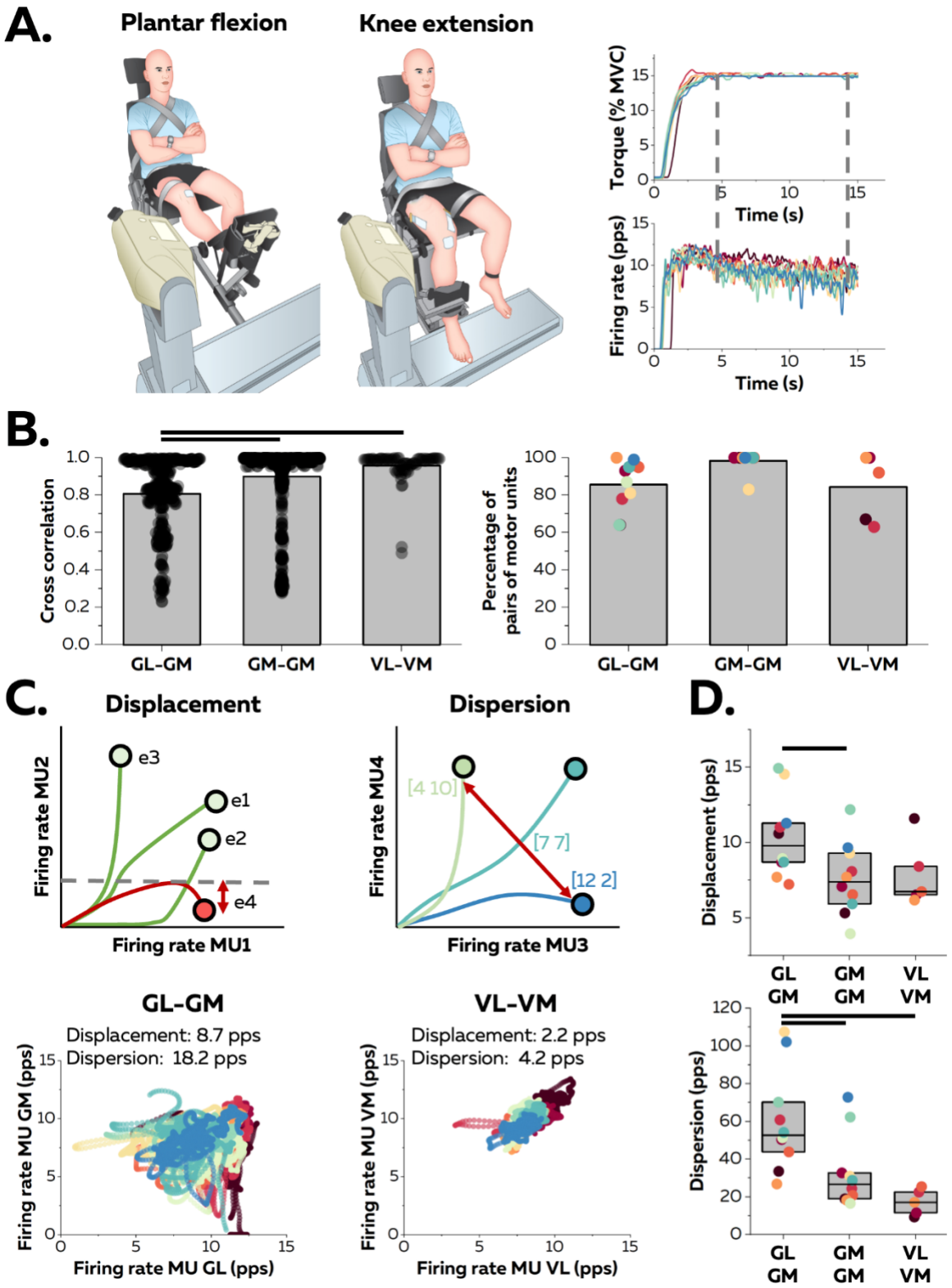

Figure 1- Motor unit behavior during the reference contractions. (A) Participants performed 10 torque-matched submaximal isometric plantar flexion or knee extension contractions. Typical traces of torque are displayed for one participant, where each line/color represents a different contraction. Electromyographic signals were recorded using surface grids of electrodes and decomposed into motor unit discharge times. Typical traces of motor unit firing rates are displayed for one motor unit, where each line/color represents a contraction. Only segments where the torque matched the target (i.e., between the dash lines) were considered for further analyses. (B, left panel) Correlation coefficients between smoothed firing rates were calculated for the pairs of motor units from the gastrocnemius

lateralis and medialis (GL-GM), from GM (GM-GM), and vastus lateralis and medialis (VL-VM). Each data point is a pair of motor units and the bar denotes the mean. (B, right panel) The percentages of pairs with a significant correlation were reported for each participant. Each data point is a participant, and the bar denotes the mean. (C) Motor unit displacement and dispersion were calculated to identify when variations in motor unit activity deviated from expected variations based on the assumption that they received a one-dimensional common input. Specifically, motor unit displacement quantifies the difference in firing rates between two motor units when the firing rates of the two units vary in opposite directions. In this example, e1, e2, and e3 show an increase in firing rate for the two motor units or an increase in firing rate for one motor unit while the other plateaus. The displacement for these three examples is equal to 0, as there are no opposite variations in firing rates. The displacement for e4 is calculated as the maximal difference between the dash line and the firing rate of MU2. Motor unit dispersion quantifies the maximal difference between the distributions of firing rates of a population of motor units for a norm value λ. In this example, we have a population of two motor units with λ equal to 14. The distribution of firing rates between the two motor units changed between trials, which opposes the hypothesis of a 1-D common input. The dispersion was calculated as the distance between the two most distant points (blue and green). Two examples of these metrics are displayed for two pairs of motor units from the GL and GM and from the VL and VM. Each line of different colors is a trial. (D) Average motor unit displacement and dispersion across participants for GL-GM, GM, and VL-VM pairs. Each data point is a participant, and the box denotes the 25th and 75th percentiles of the values distribution. The line is the median. The thick horizontal black lines denote a significant statistical difference between muscles ($p<0.05$).

Online control of motor unit firing rate

The participants were instructed to perform submaximal 15-s isometric contractions at the same intensity as the reference contractions while receiving additional visual feedback on the firing rates of two motor units (referred to as *online* contractions; Figure 2A). This visual feedback consisted of a cursor moving in a 2-D space. The coordinates of the cursor corresponded to the firing rates of two motor units. During the experiment, each motor unit was depicted on the *x* or *y* axis, independent of the recruitment threshold. However, for analysis purposes, the firing rate of the motor unit with the lowest recruitment threshold was depicted in the *x*-coordinate and the firing rate of the motor unit with the highest recruitment threshold was depicted in the *y*-coordinate. Even though differences in recruitment threshold between muscles need to be interpreted with caution due to force sharing strategies, it is worth noting that the pairs of motor units displayed to the participant in the different conditions exhibited differences in recruitment thresholds: 6.7 ± 4.2 %MVC (n=17) for GL-GM, 3.1 ± 1.7 %MVC (n=16) for GM-GM, and 2.0 ± 1.7 %MVC (n=9) for VL-VM. Two target areas along *x*- (Target 1) and *y*- axes (Target 2) were alternatively displayed to the participants (Figure 2A; see *Methods* for information about the targets). To move the cursor within these targets, the participants had to differentially change the firing rate of the two motor units (i.e., increase in one unit with no change or decrease in the other unit). After a phase of familiarization (see *Methods*), the participants were instructed to alternately reach one of the targets (five contractions for each target in a randomized order) while maintaining the target torque. The success rate was quantified as the

percentage of time spent within the required target area over the total duration of the contraction. Each participant repeated the same task with different pairs of motor units for a maximum of four pairs to avoid fatigue. The task was performed with pairs of motor units from GL and GM, pairs of motor units from GM, and pairs of motor units from VL and VM.

Three extreme scenarios were possible (Figure 2A): i) the participant failed to reach Targets 1 and 2 (success rates: 0% and 0%), ii) the participant only reached Target 1 but failed to reach Target 2 (total success rates: 100% and 0%), and iii) the participant reached Targets 1 and 2 (success rate: 100% and 100%). While the second scenario may appear as a flexible control, it corresponds to the selective recruitment of the lowest threshold motor unit (cursor in Target 1), and therefore does not provide evidence of the ability to reverse the recruitment order. In the third scenario, participants succeeded in volitionally dissociating the activity of the two motor units. Specifically, this implies that they isolated the activation of the highest threshold unit, an observation that is inconsistent with a rigid strategy that would associate a 1D common input with the size-recruitment principle. Therefore, we considered that the first two scenarios supported the presence of common synaptic inputs constraining the firing rate of the two motor units, whereas the third scenario supported the presence of different inputs to the motor units.

The success rate was compared using a linear mixed-effects model with Muscle (GL-GM, GM-GM, VL-VM) and Target (T1, T2) as the main effects and Participants as a random effect. There was a main effect of Muscle ($p<0.001$) and Target ($p=0.018$) but no interaction between Muscle and Target ($p=0.48$). Specifically, the success rate was higher for GL-GM than for both GM-GM ($p<0.001$) and VL-VM ($p=0.008$) regardless of the target. In addition, the success rate of Target 1 was higher than that of Target 2 ($p=0.018$), regardless of the Muscle (Figure 2C). Of note, four pairs of motor units from GL and GM (recorded from two participants) exhibited a success rate close to 100% for both targets, demonstrating the ability of these participants to selectively activate these units (Figure 2C). In contrast, when considering pairs of motor units from the GM or VL-VM, the success rate was close to zero for Target 2, which corresponded to a failure to selectively recruit the highest threshold unit. It is worth noting that three pairs (one for GM-GM and two for VL-VL) exhibited substantial success rates (>40%) for Target 2. However, this does not fully support a volitional independent control as the same pairs exhibited a success rate close to zero for Target 1. This can be explained by the fact that the difference in recruitment threshold between these units was very small (<2% MVC). Indeed, because of synaptic noise, the order of recruitment between units with similar recruitment thresholds may

vary across contractions [27]. It is also worth noting that some participants managed to activate only the motor unit with the lowest recruitment threshold (Target 1) but were not able to selectively activate the motor unit with the highest recruitment threshold (Target 2) (Figure 2C). As mentioned previously, this observation does not imply the presence of more than one 1-D common input. Interestingly, to selectively recruit the motor unit with the lowest threshold while maintaining the effective joint torque, the participants compensated with other muscles. For example, when feedback was provided on two GM motor units, they increased GL activation to limit the recruitment to the lowest threshold GM motor unit. Together, these results demonstrated that participants were only able to volitionally dissociate the activity of motor units from the GM and GL, which supports the assumption that motor units from the GM and GL receive at least two different inputs.

We further quantified the deviations of the cursor trajectory from a 1-D manifold by computing the motor unit displacement and dispersion during the reference contractions and the online control tasks (Figure 2D). These metrics were calculated for each pair of motor units provided as a feedback, and were compared using a linear mixed-effects model with Muscle (GL-GM; GM; VL-VM) and Task (Reference; Online) as fixed effects and Participant as a random effect. There was a significant effect of Muscle ($F=22.9$; $p<0.001$) and Task ($F=14.6$; $p<0.001$) on motor unit displacement, whereas the interaction between Muscle and Task was non-significant ($F=1.3$; $p=0.30$). Specifically, the displacement was higher during the online control contractions (8.2 ± 3.9 pps) than during the reference contractions (5.8 ± 3.4 pps; $p < 0.001$), regardless of the muscle. The displacement was also higher between motor units from GM and GL (10.2 ± 3.9 pps) than for pairs from GM (5.0 ± 1.9 pps; $p < 0.001$) and from VL-VM (5.9 ± 3.2 pps; $p = 0.015$; Figure 2D). No differences were observed between the GM-GM and VL-VM pairs ($p = 0.64$). Similarly, there was a significant effect of Muscle ($F=21.4$; $p<0.001$) and Task ($F=15.0$; $p<0.001$) on dispersion, whereas the interaction between Muscle and Task was still non-significant ($F=1.6$; $p=0.21$). The dispersion was higher during the online control task (17.0 ± 8.1 pps) than during the reference contractions (11.9 ± 6.8 pps; $p < 0.001$), and was higher between motor units from GM and GL (20.9 ± 8.0 pps) than for pairs from GM (10.5 ± 3.7 pps; $p < 0.001$) and VL-VM (12.1 ± 6.9 pps; $p = 0.013$; Figure 2D). No differences were observed between the GM-GM and VL-VM pairs ($p = 0.68$). The higher dispersion and displacement observed during the online task for VL-VM and GM-GM motor units likely indicate exploratory strategies used by the participants to dissociate the activity of these units,

while being unable to achieve the level of flexibility exhibited by the GM-GL pairs (Figure 2D) and to reach the appropriate target (Figure 2C).

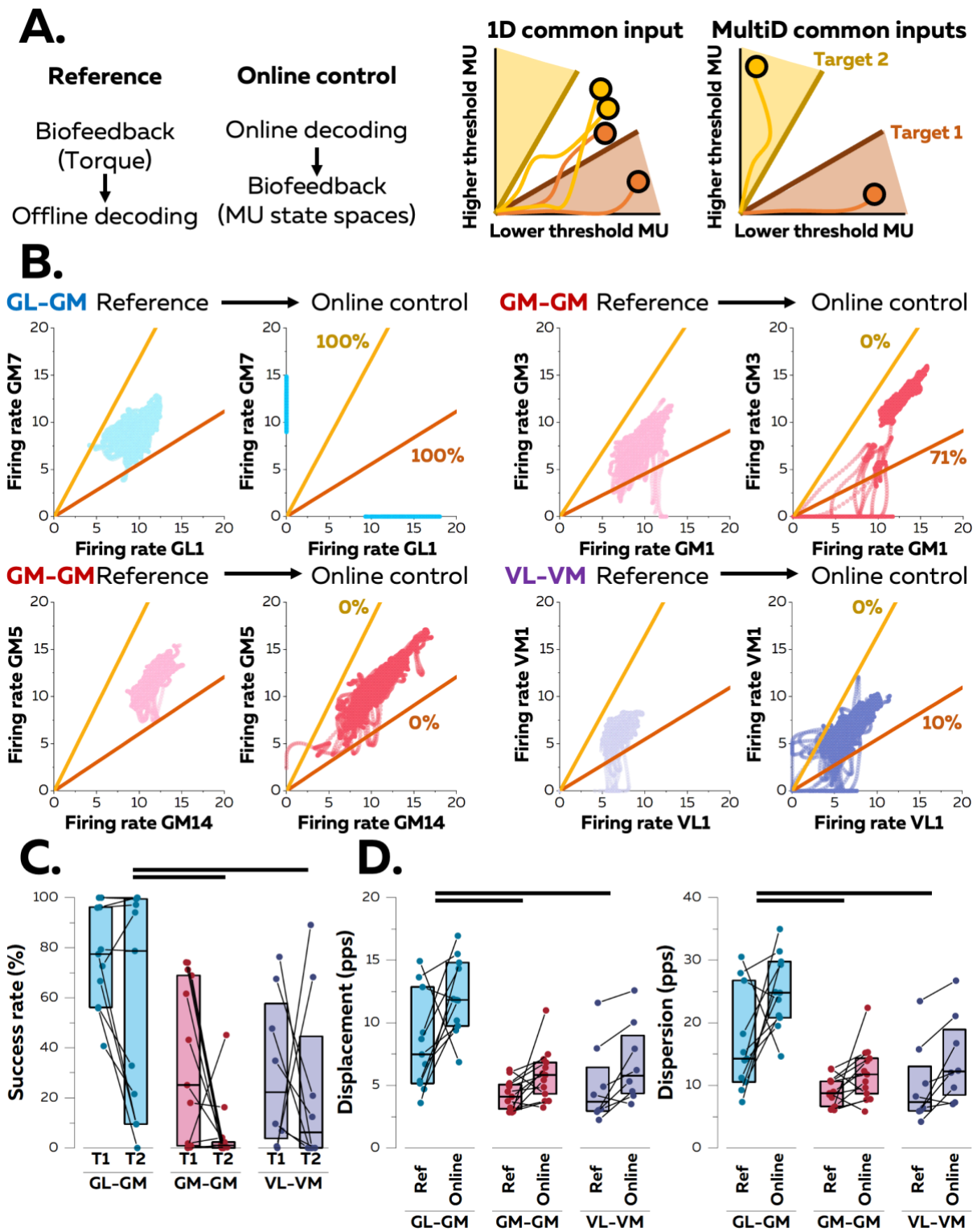

Figure 2- Volitional control of motor unit firing rates. (A) During the second part of the experiment, motor unit firing rates were decoded in real-time and converted into visual feedback displayed to the participant. The visual feedback consisted of a two-dimensional space in which a cursor moved according to the firing rates of two motor units. Two targets (Target 1 and Target 2) were alternately

displayed to the participant, who had to differentially modulate the firing rates of the two motor units to alternately move the cursor in the two targets. (B) Typical examples of cursor positions are depicted for the 10 reference contractions (only torque feedback) and the online contractions (5 for each target). The success rate is displayed for each target. It is calculated as the percentage of time spent within the target (while maintaining the torque constant) over the total duration of the trial. (C) Success rate for Targets 1 (T1) and 2 (T2). Each data point is a pair of motor units, the box denotes the 25th and 75th percentiles of the distribution of scores, and the line is the median. (D) Motor unit displacement and dispersion during reference contractions and on the trials of online control. Each data point is a pair of motor units, the box denotes the 25th and 75th percentiles of the distribution of values, and the line is the median**.** The thick horizontal black lines denote a significant statistical difference between muscles ($p<0.05$).

Behavior of motor units at the population level during the online contractions

We determined whether the dissociation of GM and GL motor unit activity imposed similar behavior on the motor units that were not displayed in the feedback, and therefore, from which activity was not constrained. Specifically, if non-displayed motor units receive common inputs with those displayed to the participants, they should exhibit similar behavior during online control contractions. This would result in a correlated activity between the displayed and non-displayed units (Figure 3A). By extension, we should also observe the same dissociation of activity at the population level as that observed at the paired level.

For each motor unit provided with feedback, we calculated the correlation between its activity and that of each non-displayed unit. This correlation was calculated between the smoothed firing rates over the 10 online contractions. Typical examples of these relationships are shown in Figure 3A, with low correlation coefficients between the displayed motor unit from the GL and all the non-displayed motor units from the GM, and high correlation coefficients between the displayed motor unit from the GM and the non-displayed motor units from the GM. A linear mixed-effects model was used to first compare the correlation coefficients, with Condition (reference; online) and Muscle (GL-GL; GL-GM; GM-GM) as fixed effects and Participants as a random effect. We found significant effects of Condition ($F=17.1$; $p<0.001$) and Muscle ($F=134.4$; $p<0.001$) with a significant interaction between Condition and Muscle ($F= 55.2$; $p<0.001$). Specifically, the correlation coefficients were significantly lower during the online control contractions than during the reference contractions for pairs of motor units from GL and GM (0.78±0.17 vs. 0.42±0.28; $p<0.001$), while they did not change for pairs from GL (0.87±0.14 vs. 0.87±0.16; $p = 1.00$) or from GM (0.89±0.18 vs. 0.90±0.12; $p = 1.00$; Figure 3B). The same analysis was performed for the pairs of motor units from VL and VM. We found significant effects of Condition ($F= 22.6$; $p<0.001$) and Muscle ($F=3.2$; $p=0.042$) but no significant interaction between Muscle and Condition ($F= 2.6$; $p=0.073$). Specifically, the correlation coefficients were lower during the online control contractions than during the

reference contractions for all the pairs of motor units. However, it is worth noting that the correlations stayed at a high level (0.98±0.02 vs. 0.89±0.14; $p<0.001$), regardless of the condition.

Overall, these results highlighted that uncoupling the firing rates of pairs of GL-GM motor units resulted in similar behaviors at the population level (Figure 3B). Notably, 81.9 ± 40.2% of the non-displayed GL-GM pairs of motor units mirrored the trend observed in the displayed GL-GM pairs of motor units. By extension, non-displayed motor unit pairs from the same muscle (GL-GL or GM-GM; Figure 3B) remained highly correlated. This behavior of non-displayed motor units demonstrates that complete independent control was not achieved at the single motor unit level and supports neural constraints at the population level. These populations were anatomically defined as those comprising motor units from the same pool.

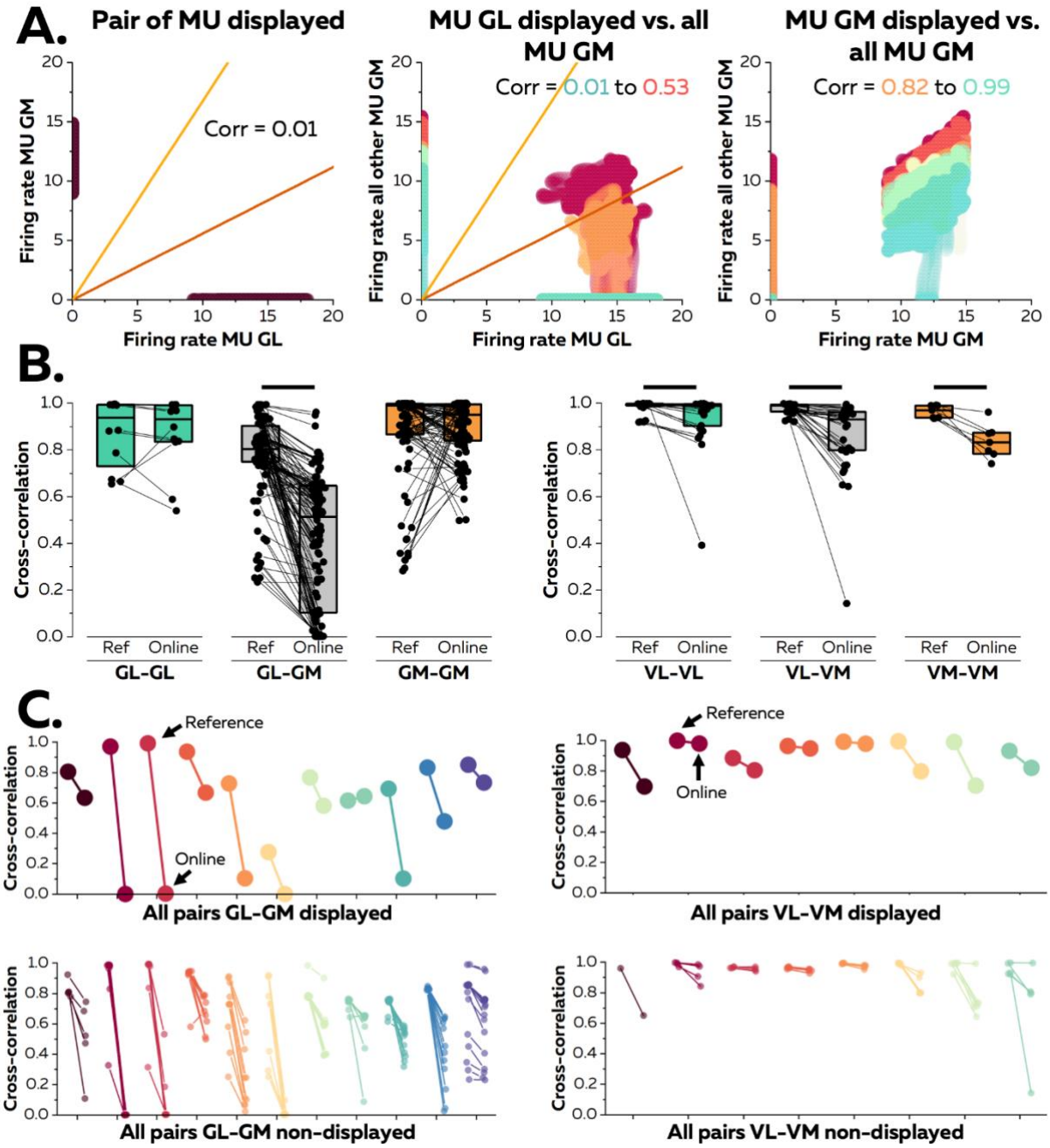

Figure 3- Changes in firing rate at the motor unit population level. (A) We calculated the correlation coefficients between the smoothed firing rates of the motor units displayed to the participant and the smoothed firing rates of the non-displayed units. In this example, the correlation coefficient between the firing rates of the two displayed motor units was 0.01 (left panel), showing a perfect dissociation of the activity of the two units. We extended the analysis to the correlation between the firing rate of the displayed motor units from the GL (central panel) or GM (right panel) and all the other motor units from GM. Each pair of motor units has a different color. (B) Correlation coefficients between the motor units (displayed and non-displayed to the participants) during the reference contractions and the online control contractions. Each data point is a pair of motor units, and the connecting line denotes the change in correlation between conditions. The box denotes the 25th and 75th percentiles of the distribution of coefficients and the black line is the median. The thick horizontal black lines represent a significant statistical difference between conditions. (C) The changes in correlations observed between reference contractions and online control trials were separated between all pairs of motor units displayed to the participant (top panel). The changes in correlations between the displayed units and those non-displayed units are shown in the bottom panel.

Strategies associated with dissociation of motor unit activity during the online task.

We examined the control strategies when the participants aimed to dissociate the activity of the motor units from the GM and GL. We used a 3D force sensor positioned at the bottom of the foot pedal to estimate the ankle moments in three axes (dorsiflexion/plantarflexion, inversion/eversion, and abduction/adduction; Figure 4). These moments were averaged during the reference contractions and the online control contractions while the cursor was in the target favoring GL recruitment (TGL), GM recruitment (TGM), or the position in between (Tgas) (Figure 4A). A linear mixed effect-models was used to compare ankle moments across conditions (Reference, TGL, TGM, Tgas) as a fixed effect and Participant as a random effect. There was no main effect of Condition on ankle moments in the Dorsiflexion/Plantarflexion ($F=0.04$; $p=0.99$) or Inversion/Eversion axes ($F=1.2$; $p=0.31$). Conversely, a significant effect of Condition was found for the ankle moment in the Abduction/Adduction axis ($F=4.1$; $p= 0.014$), showing that selectively recruiting the GM motor unit was associated with more abduction (-10.9±13.0 N.m), and conversely selectively recruiting the GL motor unit was associated with more adduction (7.4±17.7 N.m; $p=0.015$, Figure 4B). No other significant differences were observed (all $p > 0.068$).

Finally, we tested whether the participants increased the activation of their antagonist muscles (Tibialis Anterior [TA], Vastus Lateralis [VL]), which could have increased co-contraction around the ankle joint and modulated reciprocal/recurrent inhibition [28,29]. This was specifically important for distinguishing between the central and peripheral origins of the observed dissociation of the GM and GL motor units. A linear mixed-effects model was used to compare the EMG amplitude of TA and VL across Conditions (Reference, TGL, TGM, Tgas) as a fixed effect and Participant as a random effect. There was no main effect of Condition for TA ($F=2.1$; $p=0.12$) or VL ($F=0.23$; $p=0.87$; Figure 4C). This suggests that dissociation of the GL and GM motor units was achieved through different descending inputs rather than with focused inhibition.

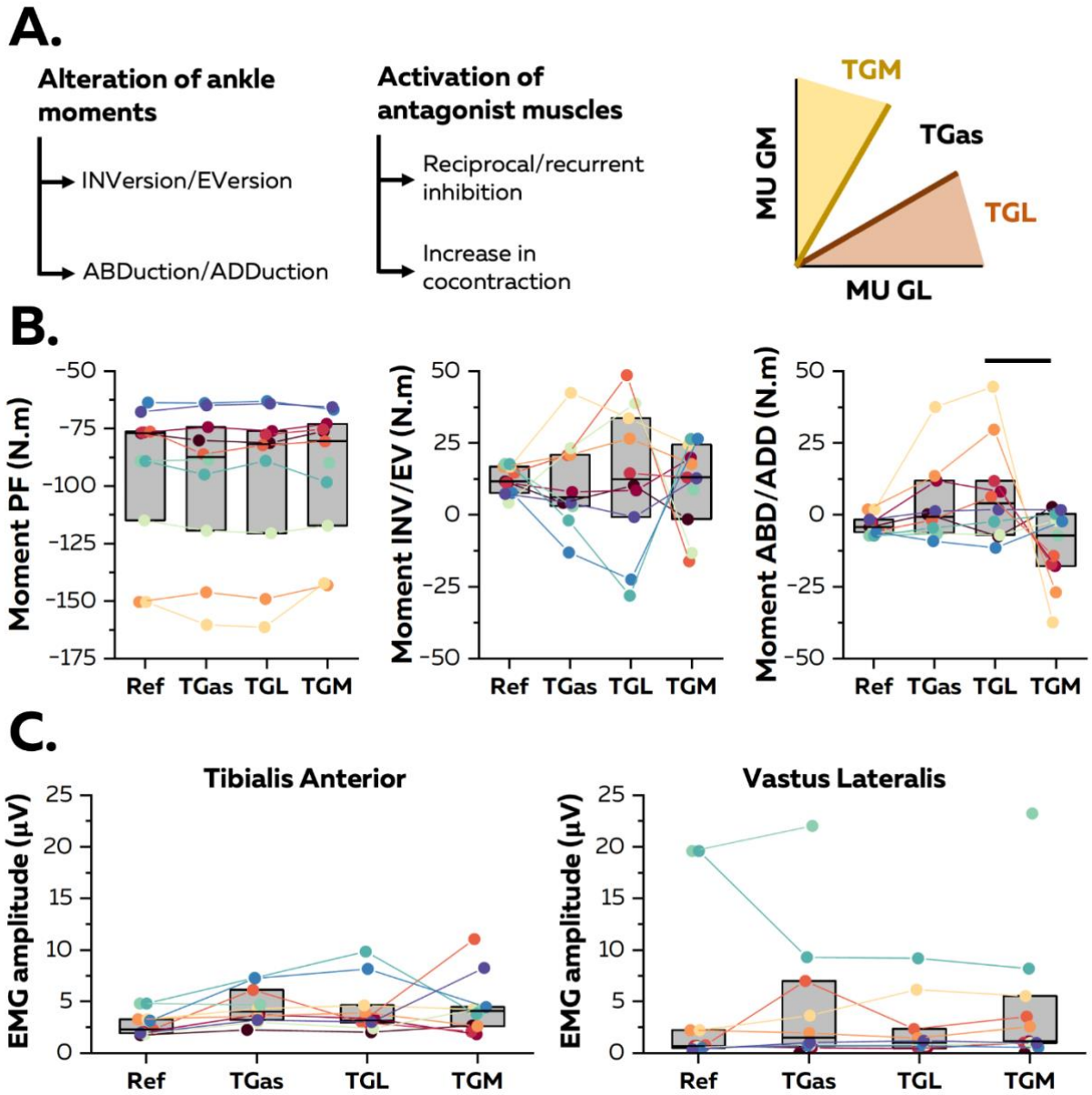

Figure 4- Control strategies during the online task. (A) To investigate the strategies associated with the dissociation of GL and GM motor unit firing rates, we identified the time stamps where the cursor was in the target favoring GL (TGL), or GM (TGM) motor unit recruitment. Tgas refers to a cursor position between the two targets. Ankle moments and EMG amplitudes of the Tibialis anterior and Vastus lateralis were averaged over these periods and compared. (B) Average ankle force moments during the reference (Ref) contractions and the three targets. Each data point is a participant and the connect lines denote the variations between conditions. The box represents the 25th and 75th percentiles of the distribution of moments and the black line is the median. (C) Each data point is a participant and the connecting lines denote the variations between conditions. The box represents the 25th and 75th percentiles of the distribution of EMG amplitudes and the black line is the median. The thick horizontal black lines represent a significant statistical difference between conditions ($p<0.05$).

Discussion.

Low-dimensional neural control of movement has been debated for decades, primarily at the muscle level. In this study, we employed a real-time feedback paradigm in which participants were asked to volitionally dissociate the firing activity of pairs of motor units. In most cases, participants were able to fully dissociate the activity of pairs of GL-GM motor units, but this strategy imposed a similar behavior at the population level, that is, dissociation of the firing rate was observed for all other GL-GM motor unit pairs that were not displayed as feedback. Conversely, volitional dissociation of firing rates was not observed between motor units of the GM muscle or between units of other anatomically defined synergist muscles (VL and VM). Together, this provides evidence that the control of motor units is constrained within low-dimensional manifolds by common inputs, thereby imposing minimal flexibility on the control of motor units. Interestingly, the number of dimensions varied between the muscle groups, despite both tasks consisting of a single mechanical degree of freedom. This suggests that the dimension of the neural control can exceed the number of mechanical degrees of freedom. These results represent a significant advancement in our understanding of the modular organization of movement at a finer scale of analysis (i.e. motor neurons) compared to previous research.

In the absence of direct measures of synaptic currents to motor neurons in humans, the correlation (or synchronization) between the firing rates of motor units has been widely used to infer the presence of common inputs [6,27,30,31]. In addition to reducing the number of degrees of freedom for movement control [32], common inputs to motor neurons also reduce the impact of synaptic noise on force output, thus directly contributing to a finer control of muscle force [7]. In this study, we observed significant correlations for most pairs of the GL-GM, GM-GM, and VL-VM motor units during the torque-matched contractions (reference contractions; Figure 1B). However, despite these significant correlations, the behavior of the motor units during the reference contractions occasionally deviated from a 1-D monotonic manifold imposed by a hypothetical 1-D common input. Larger deviations were observed for the GL-GM pairs than for GM-GM and VL-VM pairs (Figure 1B). This is consistent with the observation that most participants were able to dissociate the activity of the GL-GM motor units, even without extensive training (see *Methods*). Importantly, this dissociation involved - in some cases (n=4, Figure 2C) - volitional recruitment of the higher threshold motor unit without recruiting the lower threshold unit, providing strong evidence of independent control of GL and GM motor

units. As our results did not show consistent changes in TA or VL activity during the real-time feedback tasks (Figure 4c), we are confident that such independent control was achieved through distinct common inputs rather than focused inhibition. Indeed, inhibition could differentially affect GL and GM motor unit behavior, as suggested by Susuki et al. [28], despite receiving common descending inputs. Overall, our results strongly indicate that the GM and GL motor units are driven by at least two descending inputs, which is agreement with previous indirect observations [21,33].

Interestingly, all the motor units that we could detect from the GL and GM, but that were not used as feedback, exhibited similar behavior to their homonymous motor unit provided as feedback. In addition, the participants were unable to volitionally dissociate the activity of the GM-GM and VL-VM motor units (Figure 3). Although cortical neural substrates for the volitional selective control of motor units may exist [25], such flexible behavior was not observed when considering these pairs of motor units. Therefore, we concluded that common inputs to motor units from one or several synergistic muscles constrained their activity within low-dimensional manifolds (one or two dimensions in our tasks). This echoes previous results on a non-compartmentalized muscle (tibialis anterior), in which participants failed to volitionally control individual motor units even after weeks of training [24]. The inability to dissociate the activity of motor units from different muscles (VL-VM) was less expected given previous results reporting volitional dissociation between motor units from a bifunctional and compartmentalized muscle, such as the biceps brachii [23]. In addition, our results contrast with recent results from Del Vecchio et al. [34], which suggested the existence of two distinct synergies grouping VL and VM motor units during isometric knee extension, with some motor units from VL and VM being represented in different synergies. They also noted that some motor units from these two muscles were grouped within the same synergy. Therefore, it is possible that the lack of volitional dissociation observed in our study is explained by a selection bias of VL and VM motor units from the same synergy, therefore receiving the same descending inputs. An alternative explanation that would reconcile our observations with those of Del Vecchio et al. [34] is that 1-D common input would project to the full population of the VL and VM motor units, with heterogeneous projections of inhibitory feedback into this population, leading to decorrelated activity between some (but not all) units, and thus to the identification of multiple synergies. The impact of recurrent inhibition on the decorrelating activity of neurons receiving common excitatory inputs has been highlighted in network models [35,36]. This would explain why participants failed to volitionally dissociate the firing rate of the VL and VM motor units

despite the identification of multiple synergies [34]. Testing this hypothesis could involve manipulating inhibition by targeting specific afferent pathways (e.g., nerve endings using hypertonic saline) or modulating reciprocal inhibition. Finally, it is also important to consider that participants could have achieved GM-GM and VL-VM dissociation if provided with more exposure to the online task, although their success in dissociating the GL-GM motor units suggests that the experimental design was appropriate.

Overall, our results suggest that the firing activity of motor units from anatomically defined synergistic muscles is constrained within low-dimensional manifolds, with a varying number of dimensions depending on the joint and muscles. Interestingly, a different number of dimensions were observed even though both motor tasks (knee flexion and plantarflexion) were limited to a single mechanical degree of freedom. This result suggests that the dimensions of the manifold of control is not imposed by the number of effective mechanical degrees of freedom but may be shaped by constraints of the musculoskeletal system [37,38]. Specifically, the VL and VM motor units seem to receive common inputs, which is consistent with their role in regulating internal joint stress, requiring covariation of their activities [39]. Conversely, because GM and GL muscles have different actions in the frontal plane [40], which is supported by our data (Figure 4b), the presence of multiple motor common inputs could allow for more flexible control to comply with different task goals, such as joint stabilization. Over time, the central nervous system might compromise between various objectives, such as reducing the control dimensionality (which should involve common inputs to motor neurons) and complying with the task goals in which these muscles are involved (which would require a certain level of flexibility). Future studies should investigate the plasticity of these low-dimensional manifolds when learning new tasks or after nervous system injury.

Methods.

1. Participants and ethical approval

Ten physically active male volunteers (mean±standard deviation; age: 29.6±6.9 years, height: 179±5 cm, and body mass: 73.3±4.9 kg) participated in the triceps surae experiment, and five physically active male volunteers (age: 30.4±6.5 years, height: 176±6 cm, and body mass: 75.6±4.7 kg) participated in the quadriceps experiment. Three of them participated in both experiments. Participants had no history of lower leg pain with limited function that required time off work or physical activity, or a consultation with a health practitioner in the previous 6 months. The procedures were approved by the local ethics committee (CERNI – Nantes Université, n°04022022), and were performed according to the Declaration of Helsinki, except for registration in a database. The participants were fully informed of any risks or discomfort associated with the procedures before providing written informed consent to participate.

Notably, we specifically recruited males, as the pilot data revealed that too few (if any) GL or VM motor units could be identified with sufficient accuracy in females. This aligns with previous works showing that a greater number of motor units can be decomposed in males than in females (although the reasons for this discrepancy are yet to be well established) [41].

2. Experimental design

For the triceps surae experiment, the participants sat on a dynamometer (Biodex System 3 Pro, Biodex Medical, USA) with their hip flexed at 80°, 0° being the neutral position, and their right leg fully extended (Figure 1A). Their ankle angle was set to 10° of plantarflexion, 0° being the foot perpendicular to the shank. For the quadriceps experiment, the participants sat on the dynamometer with their hips flexed at 80° and the knee of their right leg flexed at 80°, 0° being the full extension (Figure 1A). Inextensible straps were tightened during both tasks to immobilize the torso, pelvis, and thighs on the test side. Each experiment involved a single experimental session lasting approximately 3 h.

The protocol was the same, regardless of the experiment (triceps surae or quadriceps). The experimental session began with a standardized warm up, which included five 3-s isometric contractions at 50%, 60%, 70%, and 80% and three 3 s contractions at 90% of the participants' subjective maximal torque. After 2 min of rest, the participants performed three MVCs for 3 s, with 60 s of rest in between. Peak MVC torque was considered as the maximal value obtained

from a moving average window of 250 ms. Participants then performed one trapezoid isometric contraction (10 s ramp up, 30 s plateau, and 10 s ramp down) at a submaximal torque to identify motor unit filters offline (referred to as "baseline" contractions). For the triceps surae protocol, the torque level was chosen on an individual basis based on the number of identified motor units. Specifically, in some participants, the GL muscle was minimally activated at the lowest torque levels (15% and 20% MVC), leading to no or a few identified motor units. In this case, a higher torque level (20 or 25% MVC) was tested. The retained torque was 15% MVC for five participants, 20% MVC for four participants, 25% MVC for one participant. This torque level was then kept the same during the whole experimental session. For the quadriceps protocol, the torque level was set at 10% MVC as it was sufficient to recruit motor units in both muscles. The choice of a relatively low torque level was also motivated by the need to limit fatigue, which develops faster during knee extension than plantarflexion [42]. After a 15-30 min rest period during which automatic decomposition and manual editing of the motor units were performed, the participants performed ten submaximal isometric contractions for 15 s, with 15 s of rest in between. Only torque feedback was provided to the participants during these contractions (referred to as "reference" contractions) so that they could be used to assess the "natural" motor unit recruitment strategies.

The rest of the experimental session consisted of two to four blocks of a series of submaximal isometric contractions during which the participants were instructed to dissociate the activity of two motor units while keeping the plantarflexion torque constant. Specifically, participants navigated a cursor in a 2D space were the *x*- and *y*- axes represented the firing rate of motor units #1 and #2. The scale of each axis was set up from 0 to a maximum of two times the mean firing rate of the corresponding motor unit measured during the baseline contraction. This ensured that the cursor was not biased toward any of the axes during natural contractions. A real-time feedback of torque output was also provided to the participants in the form of a vertical gauge that the participants had to keep between two lines representing ±5% of the target torque. For the triceps surae protocol, we aimed to provide visual feedback of four different pairs of motor units for each participant: two pairs composed of motor units of both the GM and GL (between-muscle pairs) and two pairs composed of motor units of the GM (within-muscle pairs). For the quadriceps experiment, we aimed to provide visual feedback on two different pairs of motor units composed of the motor units of both the VM and VL (between-muscle pairs). Each pair was tested separately within a block of contractions as described below. Of note, because of either a decrease in the accuracy of motor unit identification during the

experiment or the overall long duration that made the lower limb position progressively uncomfortable, we tested fewer pairs of motor units (mean number of tested pairs for each participant: 3.3 ± 0.9 pairs [total = 17 for GM-GL and 16 for GM-GM] for the triceps surae experiment and 1.8 ± 0.4 pairs [total=9] for the quadriceps experiment). Notably, the nine pairs for the quadriceps experiment originated from five participants because a drastic drop in the decomposition accuracy across the experiment was observed for three participants.

Each block started with an exploration phase during which the participants were instructed to navigate the cursor inside the 2D space during three 60 s periods, with 60 s of rest in between. During this exploration phase, participants were asked to explore the entire 2D space; that is, to alternately move the cursor close towards (or on) the *x* and *y* axis while maintaining the plantarflexion torque at the predetermined torque target (see above). Notably, to move the cursor close to an axis (either *x* or *y*), the participants had to differentially change the firing rate of the two motor units (i.e., an increase in one unit with no change or a decrease in the other unit). For the subsequent contractions, the target spaces were added to the 2D space. These targets were in the shape of a triangle with one corner on the coordinate origin and two sides being one axis (*x* or *y*), and a line forming an angle of 30° with this axis (Figure 2A). First, participants performed a series of ten 15 s contractions during which they were asked to move the cursor in the target space close to one of the axes (*x* or *y*). The participants then performed another series of ten 15 s contractions during which they were asked to move the cursor in the target space close to the other axis. Finally, they performed a last series of ten 15 s contractions during which they were asked to move the cursor in the target space close to either the *x* axis (five contractions) or the *y* axis (five contractions). During the last series, the order of the target presentation (i.e., *x* or *y*) was randomized and unknown to the participants. The contractions were interspaced by a 14-s recovery period and the three series were interspaced by a 2 min rest period. The participants were informed that a successful trial was one in which the cursor stayed in the target space while producing the required torque, and that the ultimate objective was to move the cursor on the x or y axis, meaning that they kept one motor unit active while keeping the other motor unit off. Of note, for the purpose of this study only the third series of 10 contractions was analyzed (referred to as "online" contractions in the *Results* section), the previous series being considered as training.

3. High-density surface electromyographic recordings

For the triceps surae experiment, HDsEMG signals were recorded from four lower limb muscles: GM, GL, Tibialis anterior (TA), and VL. The TA and VL muscles were recorded to explore possible strategies for modulating the activity of the gastrocnemius motor units, such as reciprocal inhibition. Indeed, the TA and VL act as antagonists of the gastrocnemius in two main functions, i.e., plantarflexion for TA and knee flexion for VL. This was further motivated by a previous study that showed that adding knee extensor activity to plantar flexion led to a differential change in activation of the GM and GL muscles [28]. For the quadriceps experiment, signals were recorded from two lower limb muscles: the VM and VL.

A two-dimensional adhesive grid of 64 electrodes (13×5 electrodes with one electrode absent in a corner, gold-coated, inter-electrode distance: 8 mm; [GR08MM1305, OT Bioelettronica, Italy]) was placed over each muscle. Before electrode application, the skin was shaved and cleaned with an abrasive gel (Nuprep, Weaver and company, USA). The adhesive grids were held on the skin using semi-disposable bi-adhesive foam layers (OT Bioelettronica, Italy). Skin-electrode contact was ensured by filling the cavities of the adhesive layers with a conductive paste. A 10-cm-wide elastic band was placed over the electrodes with a slight tension to ensure that all the electrodes remained in contact with the skin throughout the experiment. A strap electrode dampened with water was placed around the contralateral ankle (ground electrode) and a reference electrode (5 × 5 cm, Kendall Medi-Trace™, Canada) was positioned over the tibia (triceps surae experiment) or the patella (quadriceps experiment) of the ipsilateral limb. The EMG signals were recorded in monopolar mode, bandpass filtered (10-500 Hz) and digitized at a sampling rate of 2048 Hz using a multichannel acquisition system (EMG-Quattrocento; 400-channel EMG amplifier, OT Biolelettronica, Italy).

We used an open-source software developed and validated by our team to decompose the EMG signals in real-time [26]. First, EMG signals were recorded during a submaximal contraction, such that channels with artifacts and low signal-to-noise ratio could be removed from all further analyses. Second, the EMG signals collected during the baseline contraction were decomposed offline using a blind-source separation algorithm [43]. This baseline contraction aimed to identify the separation vectors (motor unit filters). As highlighted in our previous validation work [26], the accuracy of the online decomposition can be improved by manually editing the offline decomposition results. Therefore, we performed a manual editing step that consisted of i) removing the spikes close to the noise level, ii) recalculating the motor-unit filter and reapplying it over the signal, iii) adding new spikes recognized as motor unit firings, and iv) recalculating

the motor-unit filter (Hug et al., 2021). For the contractions requiring real-time decomposition, EMG signals were transmitted by packages of 256 data points (125 ms with a sampling frequency of 2048 Hz), and the motor unit filters were applied over the incoming segments of the EMG signals. In addition of the incompressible delay of 125 ms, the computational time required by the software to display visual feedback is typically less than 15 ms [26].

4. Force measurements.

A dynamometer (Biodex System 3 Pro, Biodex Medical, USA) was equipped with a six-axis force sensor (Sensix, France). Even though the real-time feedback provided during the experiment was based only on either the effective plantarflexion or knee extension torque, we considered the two other torque components (abduction/adduction and inversion/eversion) in the analysis to determine whether the dissociation of motor unit activity was associated with changes in mechanical output. These mechanical signals were digitized at a sampling rate of 2048 Hz using a multichannel acquisition system similar to that used for HDsEMG (EMG-Quattrocento; 400-channel EMG amplifier, OT Biolelettronica, Italy).

5. Data analysis

Offline manual editing

To address the aims of this study, we analyzed a series of 10 reference contractions (with torque feedback only) and a series of 10 ten online contractions in which participants were instructed to move the cursor in the target space close to either the *x* axis (five contractions) or the *y* axis (five contractions). We identified 10.6 ± 3.8 (GM), 3.4 ± 1.5 (GL), 6.0 ± 1.9 (VL), and 2.2 ± 0.7 (VM) motor units per participant for the reference contractions and 9.8 ± 4.2 (GM), 2.1 ± 1.0 (GL), 4.8 ± 1.2 (VL), and 1.8 ± 0.8 (VM) motor units per participant for the online contractions. Notably, we not only analyzed the pairs of units used for the feedback, but also analyzed all the motor units that were identified during the baseline contraction. Each motor unit spike train was manually edited as described above. Notably, this manual step is highly reliable across operators (Hug et al., 2021).

Correlation between smoothed motor unit firings

We calculated the correlation coefficient between the motor unit smoothed firing rates over the 10 concatenated contractions (either the reference or the online contractions) using a cross-correlation function (max lag = 100 ms). Specifically, for each motor unit, the spike times were

first converted into continuous binary signals with 'ones' corresponding to the firing instances. The smoothed firing rate was obtained by convolving the binary vectors with a Hanning window of 400 ms. Maximum cross-correlation coefficients were considered. A significance threshold was defined for each pair of motor units as the 95th percentile of the cross-correlation coefficient distribution generated with 100 resampled versions of the two motor unit spike trains. For each motor unit, we generated a synthetic spike train by bootstrapping the inter-spike intervals (random sampling with replacement). This synthetic spike train had the same number of spikes, and the same firing rate (mean ± SD) as the original motor unit spike train.

Motor unit displacement and dispersion

We calculated two metrics proposed by Marshall et al. [25] to determine whether the firing rates of motor unit populations deviated from the expected variations, based on the assumption that they exclusively received a 1-D common input: *motor unit displacement* and *dispersion* (Figure 1C). The firing rates of a population of motor units receiving a 1-D common input should constantly vary along a 1-D monotonic manifold in the same direction as the common input. If the firing rate of one motor unit increases, all the other firing rates should either increase (e1 in Figure 1C), remain at 0 owing to a later recruitment threshold (e2 in Figure 1C), or plateau at the same value owing to rate saturation (e3 in Figure 1C). The *motor unit displacement* quantifies the difference in firing rates between two motor units when the firing rates of the two units vary in opposite directions (e4 in Figure 1C). For this, we first computed the maximum non-negative changes in the firing rates between two timestamps, *t* and *t'*, for a population of *n* motor units:

$$\Delta r(t,t') = max\left(r_{1,t} - r_{1,t'},\ r_{2,t} - r_{2,t'}, \dots,\ r_{n,t} - r_{n,t'}\right)$$

If all the motor unit firing rates vary in the same direction, then either $\Delta r(t,t')$ or $\Delta r(t',t)$ should be equal to 0. The displacement $d(t)$ was considered as the minimum value between $\Delta r(t,t')$ and $\Delta r(t',t)$. It is worth noting that we quantified the displacement values while iteratively adding a time lag τ and τ' of up to 25 ms to *t* and *t'*, respectively, to account for differences in conduction velocities between motor neurons. Therefore, we kept the minimal displacement value between $\Delta r(t+\tau, t'+\tau')$ and $\Delta r(t'+\tau', t+\tau)$. Finally, we considered the displacement *d* for a population of motor units as the maximum value out of all the time stamps *t*.

The *dispersion* quantifies the maximal deviation of variations in firing rates from a 1D manifold at the population level. Thus, the summed firing rates of a population of motor units receiving a 1-D common input, equivalent to its L1-norm $\|r\|$, should always be associated with the same population state, that is, the distribution of firing rates within the population. Any change in L1-norm within a population of motor units for a given norm value λ would mean that at least two motor units have different firing rates for the same summed firing rate. The *dispersion* quantifies the maximal difference between L1-norms for a given norm value λ (λ= 14 in Figure 1C).

$$disp(\lambda) = \max([\![r_{t_1} - r_{t_2}]\!])$$

We also quantified the dispersion values while iteratively adding time lag vectors τ and τ' of up to 25 ms to the population of motor units.

Volitional dissociation of motor unit activity

To determine whether the participants were able to dissociate the activity of motor units, we calculated the success rate as the percentage of time spent within the required target area out of the total duration of the contraction. Notably, only data obtained while the participants reached the target +/- 5% were considered in this calculation.

EMG amplitude

To estimate the activation level of the TA and VL muscles during the triceps surae experiment, the 64 EMG signals recorded in a monopolar configuration were differentiated along the column direction to obtain 59 single-differential signals. The average rectified values (ARV) of each signal were estimated over a sliding window of 250 ms. The ARV of the 59 channels were finally averaged at each timestamp. ARV were averaged while each participant reached that target favoring the recruitment of motor units from the GL, from GM, or in between.

References.

1 Sherrington, C. S. *The integrative action of the nervous system*. (New Haven, 1906).

2 Gesslbauer, B. *et al.* Axonal components of nerves innervating the human arm. *Ann Neurol* **82**, 396-408 (2017). https://doi.org:10.1002/ana.25018

3 Bernstein, N. A. *On the Construction of Movements*. (Medgiz, 1947).

4 Latash, M. L. Understanding and Synergy: A Single Concept at Different Levels of Analysis? *Front Syst Neurosci* **15**, 735406 (2021). https://doi.org:10.3389/fnsys.2021.735406

5 Gallego, J. A., Perich, M. G., Miller, L. E. & Solla, S. A. Neural Manifolds for the Control of Movement. *Neuron* **94**, 978-984 (2017). https://doi.org:10.1016/j.neuron.2017.05.025

6 De Luca, C. J. & Erim, Z. Common drive of motor units in regulation of muscle force. *Trends Neurosci* **17**, 299-305 (1994). https://doi.org:10.1016/0166-2236(94)90064-7

7 Farina, D. & Negro, F. Common synaptic input to motor neurons, motor unit synchronization, and force control. *Exerc Sport Sci Rev* **43**, 23-33 (2015). https://doi.org:10.1249/JES.0000000000000032

8 De Luca, C. J. & Erim, Z. Common drive in motor units of a synergistic muscle pair. *J Neurophysiol* **87**, 2200-2204 (2002). https://doi.org:10.1152/jn.00793.2001

9 Gibbs, J., Harrison, L. M. & Stephens, J. A. Organization of inputs to motoneurone pools in man. *J Physiol* **485 (Pt 1)**, 245-256 (1995). https://doi.org:10.1113/jphysiol.1995.sp020727

10 Laine, C. M., Martinez-Valdes, E., Falla, D., Mayer, F. & Farina, D. Motor Neuron Pools of Synergistic Thigh Muscles Share Most of Their Synaptic Input. *J Neurosci* **35**, 12207-12216 (2015). https://doi.org:10.1523/JNEUROSCI.0240-15.2015

11 Tanzarella, S., Muceli, S., Santello, M. & Farina, D. Synergistic Organization of Neural Inputs from Spinal Motor Neurons to Extrinsic and Intrinsic Hand Muscles. *J Neurosci* **41**, 6878-6891 (2021). https://doi.org:10.1523/JNEUROSCI.0419-21.2021

12 Hug, F., Avrillon, S., Sarcher, A., Del Vecchio, A. & Farina, D. Correlation networks of spinal motor neurons that innervate lower limb muscles during a multi-joint isometric task. *J Physiol* (2022). https://doi.org:10.1113/JP283040

13 Rodriguez-Falces, J., Negro, F. & Farina, D. Correlation between discharge timings of pairs of motor units reveals the presence but not the proportion of common synaptic input to motor neurons. *J Neurophysiol* **117**, 1749-1760 (2017). https://doi.org:10.1152/jn.00497.2016

14 Binder, M. D., Powers, R. K. & Heckman, C. J. Nonlinear Input-Output Functions of Motoneurons. *Physiology (Bethesda)* **35**, 31-39 (2020). https://doi.org:10.1152/physiol.00026.2019

15 Bizzi, E. & Cheung, V. C. The neural origin of muscle synergies. *Front Comput Neurosci* **7**, 51 (2013). https://doi.org:10.3389/fncom.2013.00051

16 Ronzano, R., Lancelin, C., Bhumbra, G. S., Brownstone, R. M. & Beato, M. Proximal and distal spinal neurons innervating multiple synergist and antagonist motor pools. *Elife* **10** (2021). https://doi.org:10.7554/eLife.70858

17 Takei, T., Confais, J., Tomatsu, S., Oya, T. & Seki, K. Neural basis for hand muscle synergies in the primate spinal cord. *Proc Natl Acad Sci U S A* **114**, 8643-8648 (2017). https://doi.org:10.1073/pnas.1704328114

18 Henneman, E. Relation between size of neurons and their susceptibility to discharge. *Science* **126**, 1345-1347 (1957). https://doi.org:10.1126/science.126.3287.1345

19 Todorov, E. Optimality principles in sensorimotor control. *Nat Neurosci* **7**, 907-915 (2004). https://doi.org:10.1038/nn1309
20 Todorov, E. & Jordan, M. I. Optimal feedback control as a theory of motor coordination. *Nat Neurosci* **5**, 1226-1235 (2002). https://doi.org:10.1038/nn963
21 Levine, J., Avrillon, S., Farina, D., Hug, F. & Pons, J. L. Two motor neuron synergies, invariant across ankle joint angles, activate the triceps surae during plantarflexion. *J Physiol* **601**, 4337-4354 (2023). https://doi.org:10.1113/JP284503
22 Basmajian, J. V. Control and training of individual motor units. *Science* **141**, 440-441 (1963). https://doi.org:10.1126/science.141.3579.440
23 Formento, E., Botros, P. & Carmena, J. M. Skilled independent control of individual motor units via a non-invasive neuromuscular-machine interface. *J Neural Eng* **18** (2021). https://doi.org:10.1088/1741-2552/ac35ac
24 Bracklein, M. *et al.* The control and training of single motor units in isometric tasks are constrained by a common input signal. *Elife* **11** (2022). https://doi.org:10.7554/eLife.72871
25 Marshall, N. J. *et al.* Flexible neural control of motor units. *Nat Neurosci* (2022). https://doi.org:10.1038/s41593-022-01165-8
26 Rossato, J. *et al.* I-Spin live: An open-source software based on blind-source separation for decoding the activity of spinal alpha motor neurons in real-time. *eLife* (2023). https://doi.org:10.7554/eLife.88670.1
27 Heckman, C. J. & Enoka, R. M. Motor unit. *Compr Physiol* **2**, 2629-2682 (2012). https://doi.org:10.1002/cphy.c100087
28 Suzuki, T., Chino, K. & Fukashiro, S. Gastrocnemius and soleus are selectively activated when adding knee extensor activity to plantar flexion. *Hum Mov Sci* **36**, 35-45 (2014). https://doi.org:10.1016/j.humov.2014.04.009
29 Yavuz, U. S., Negro, F., Diedrichs, R. & Farina, D. Reciprocal inhibition between motor neurons of the tibialis anterior and triceps surae in humans. *J Neurophysiol* **119**, 1699-1706 (2018). https://doi.org:10.1152/jn.00424.2017
30 Keen, D. A. & Fuglevand, A. J. Common input to motor neurons innervating the same and different compartments of the human extensor digitorum muscle. *J Neurophysiol* **91**, 57-62 (2004). https://doi.org:10.1152/jn.00650.2003
31 McIsaac, T. L. & Fuglevand, A. J. Motor-unit synchrony within and across compartments of the human flexor digitorum superficialis. *J Neurophysiol* **97**, 550-556 (2007). https://doi.org:10.1152/jn.01071.2006
32 Hug, F., Avrillon, S., Ibanez, J. & Farina, D. Common synaptic input, synergies and size principle: Control of spinal motor neurons for movement generation. *J Physiol* **601**, 11-20 (2023). https://doi.org:10.1113/JP283698
33 Hug, F., Del Vecchio, A., Avrillon, S., Farina, D. & Tucker, K. Muscles from the same muscle group do not necessarily share common drive: evidence from the human triceps surae. *J Appl Physiol (1985)* **130**, 342-354 (2021). https://doi.org:10.1152/japplphysiol.00635.2020
34 Del Vecchio, A. *et al.* The Forces Generated by Agonist Muscles during Isometric Contractions Arise from Motor Unit Synergies. *J Neurosci* **43**, 2860-2873 (2023). https://doi.org:10.1523/JNEUROSCI.1265-22.2023
35 Bernacchia, A. & Wang, X. J. Decorrelation by recurrent inhibition in heterogeneous neural circuits. *Neural Comput* **25**, 1732-1767 (2013). https://doi.org:10.1162/NECO_a_00451
36 Renart, A. *et al.* The asynchronous state in cortical circuits. *Science* **327**, 587-590 (2010). https://doi.org:10.1126/science.1179850

37 Ting, L. H. *et al.* Neuromechanical principles underlying movement modularity and their implications for rehabilitation. *Neuron* **86**, 38-54 (2015). https://doi.org:10.1016/j.neuron.2015.02.042
38 Tresch, M. C. & Jarc, A. The case for and against muscle synergies. *Curr Opin Neurobiol* **19**, 601-607 (2009). https://doi.org:10.1016/j.conb.2009.09.002
39 Alessandro, C. *et al.* Coordination amongst quadriceps muscles suggests neural regulation of internal joint stresses, not simplification of task performance. *Proc Natl Acad Sci U S A* **117**, 8135-8142 (2020). https://doi.org:10.1073/pnas.1916578117
40 Lee, S. S. & Piazza, S. J. Inversion-eversion moment arms of gastrocnemius and tibialis anterior measured in vivo. *J Biomech* **41**, 3366-3370 (2008). https://doi.org:10.1016/j.jbiomech.2008.09.029
41 Del Vecchio, A. *et al.* Tutorial: Analysis of motor unit discharge characteristics from high-density surface EMG signals. *J Electromyogr Kinesiol* **53**, 102426 (2020). https://doi.org:10.1016/j.jelekin.2020.102426
42 Rossato, J. *et al.* Less common synaptic input between muscles from the same group allows for more flexible coordination strategies during a fatiguing task. *J Neurophysiol* **127**, 421-433 (2022). https://doi.org:10.1152/jn.00453.2021
43 Negro, F., Muceli, S., Castronovo, A. M., Holobar, A. & Farina, D. Multi-channel intramuscular and surface EMG decomposition by convolutive blind source separation. *J Neural Eng* **13**, 026027 (2016). https://doi.org:10.1088/1741-2560/13/2/026027